

Supplemental Information

Effects of Burning and Photochemical Degradation of Macondo Surrogate Oil on its Composition and Toxicity

*Pamela P. Benz,¹ Phoebe Zito,² Ed Osborn,² Aleksandar I. Goranov,³ Patrick G. Hatcher,³ Matthew D. Seivert,⁴ Wade H. Jeffrey⁵

¹Department of Chemistry, University of West Florida, 11000 University Parkway, Pensacola, FL 32514

²Department of Chemistry, Chemical Analysis & Mass Spectrometry Facility, University of New Orleans, New Orleans, LA 70148

³Department of Chemistry and Biochemistry, Old Dominion University, Norfolk, VA 23529, USA.

⁴Department of Chemistry, University of Georgia, 140 Cedar Street, Athens, GA 30602-5028

⁵Center for Environmental Diagnostics and Bioremediation, University of West Florida, 11000 University Parkway, Pensacola, FL 32514

*corresponding author - Email: pamelabenz@uwf.edu

Number of Figures: 7

Number of Tables: 2

FT-ICR MS analysis of oils

Sample Preparation: For negative-ion electrospray ionization (neg-ESI) FT-ICR MS analysis, oil samples were dissolved in toluene to yield stock solutions (1 mg/mL) and further diluted in toluene with equal parts (v/v) methanol spiked with 0.25% (by volume) tetramethylammonium hydroxide (TMAH) to final concentration (10-50 µg/mL) before analysis.

9.4 T FT-ICR Mass Spectrometer: Whole and burned Surrogate crude oils were analyzed with a custom-built FT-ICR mass spectrometer equipped with a modular ICR data station.¹ Sample solutions were infused via a micro-electrospray source (50 µm i.d. fused silica emitter) at 0.5 µL/min by a syringe pump. Conditions for negative ion formation were emitter voltage, -2.7 kV; heated metal capillary -250V and heated to 110 °C. Ions generated by the ESI source were transferred from atmospheric pressure to the first pumping stage of the mass spectrometer through a home-built dual ion funnel assembly, developed initially at Pacific Northwest National Laboratory to increase ion transmission efficiency. The dc voltages applied on funnel 1 are -100 V and -70 V, and on funnel 2 are -40 V and -10 V. Positive ion formation occurred at the same conditions as for negative ions, but with positive values.

ICR time-domain transients were collected from a 7-segment open cylindrical cell with capacitively coupled excitation electrodes based on the Tolmachev configuration. Seventy-five individual acquisitions of 5.6 – 6.1s transient for each WSO sample were averaged, Hanning apodized, and zero-filled once before fast Fourier transformation. Broadband phase correction was applied to all mass spectra to increase resolving power by a factor of up to 2 to the conventional magnitude-mode resolving power.

ICR frequencies were converted to ion masses based on the quadrupolar trapping potential approximation. Each m/z spectrum was internally calibrated based on an abundant

homologous alkylation series differing in mass by integer multiples of 14.01565 Da (mass of a CH₂ unit) confirmed by isotopic fine structure based on the “walking” calibration equation. Experimentally measured masses were converted from the International Union of Pure and Applied Chemistry (IUPAC) mass scale to the Kendrick mass scale to identify homologous series for each heteroatom class. Peak assignments were performed by Kendrick mass defect analysis as previously described.¹ For each elemental composition, C_cH_hN_nO_oS_s, the heteroatom class, type (double bond equivalents, DBE = number of rings plus double bonds involving carbon), and carbon number, c, were tabulated for the subsequent generation of heteroatom class relative abundance distributions and graphical DBE vs. carbon number images. Formula assignments and spectra calibration were performed with in-house Predator software provided by Florida State University.^{1,2} EnviroOrg software was used to assign molecular formula. Four van Krevelen plots were constructed from FT-ICR MS-derived data to observe the changes in the molecular-level composition of the non-dispersed and dispersed oil.^{3,4} Python software to construct van Krevelen diagrams was provided by Hemingway.⁵

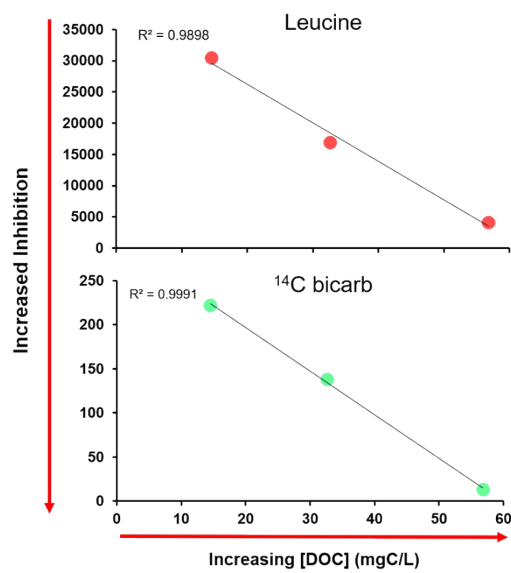


Figure S1: Correlation between toxicity (increased inhibition) and DOC concentration.

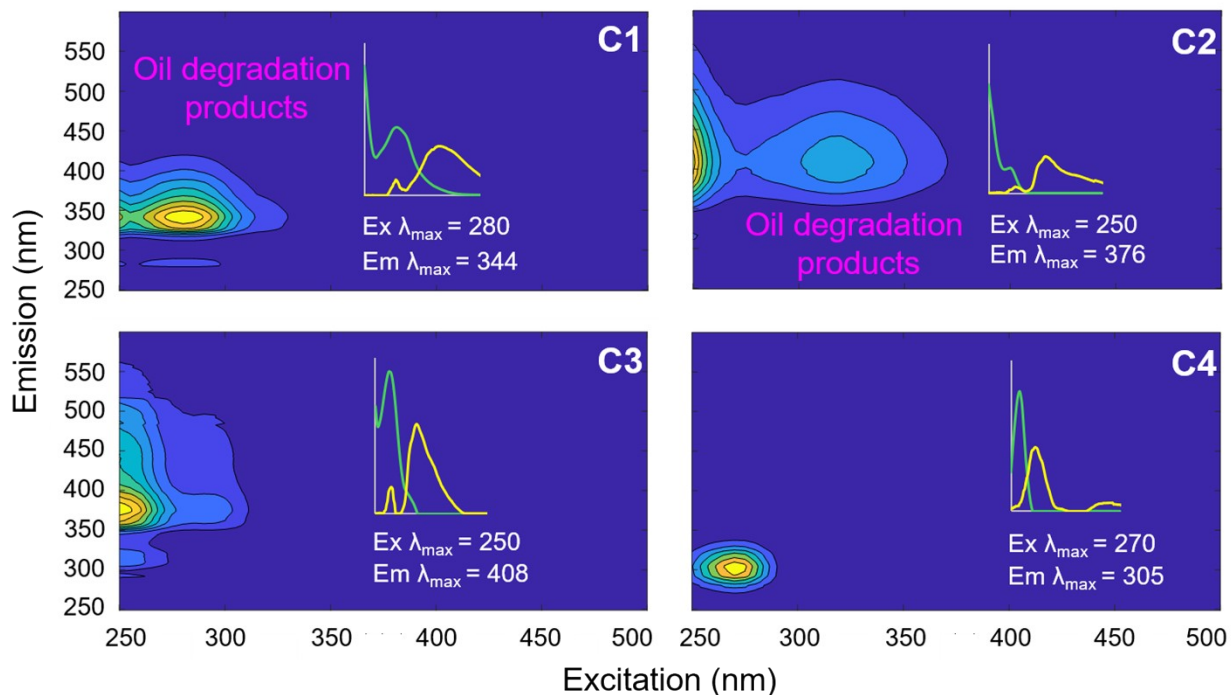


Figure S2: Fluorescence excitation emission matrix (EEMs) plots for fluorescent components 1-4 (C1-C4) determined using parallel factor analysis (PARAFAC) deconvolution.

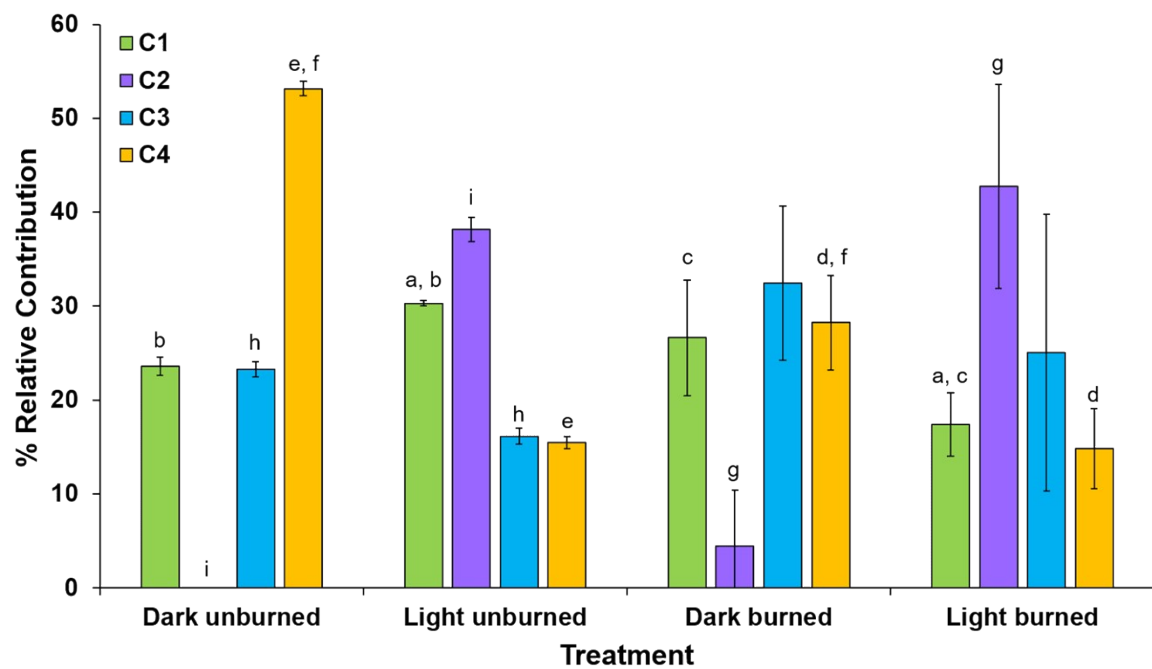


Figure S3: Percent relative contribution of fluorescent components C1-C4 in water accommodated fractions (WAF) of oil samples. The letters associated with each component (a-f) signify the treatments that are statistically different - a, b, d - i ($p < 0.001$) and c ($p < 0.05$).

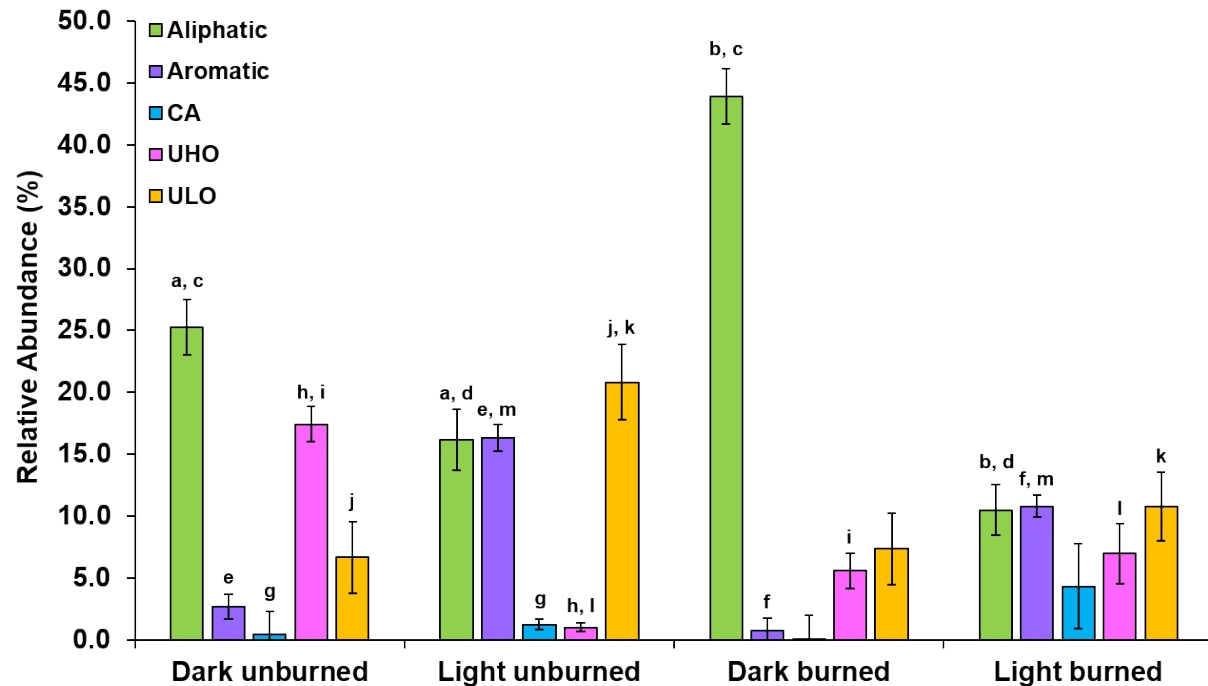


Figure S4: Bar graph of molecular formula classifications for water accommodated fractions data derived from neg-ESI FT-ICR MS. Standard deviation (SD) for the darks was propagated based on the mean SD of all replicates for each class and treatment. The letters associated with each component (a-m) signify the treatments that are statistically different - b, c, e, f, h, i, m ($\rho < 0.001$) and a, d, g, j, k, l ($\rho < 0.05$).

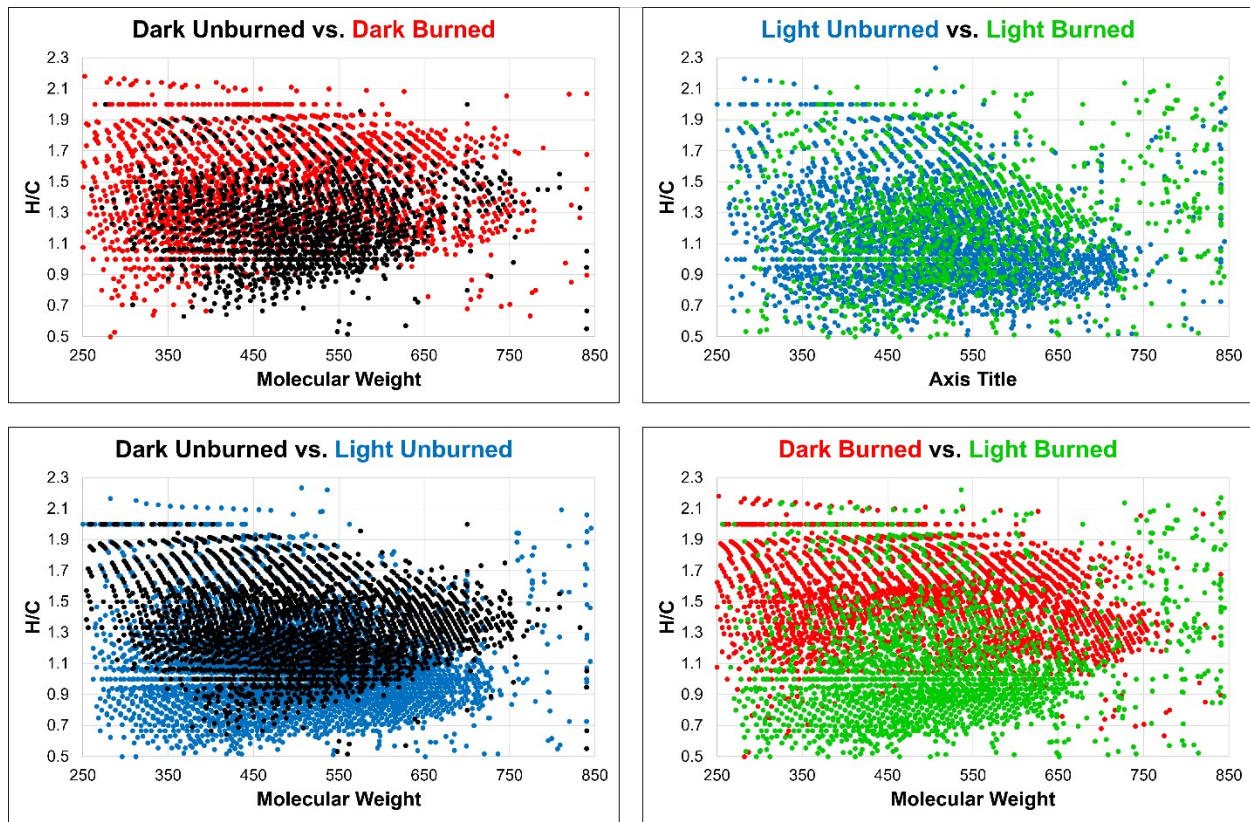


Figure S5: H/C versus molecular weight plots of molecular compositions compared based on burning (top panels) and sunlight exposure (bottom panels). Plotted formulas are only the unique ones per each sample among the two being compared.

Molecular Level Characterization of burned and unburned oil

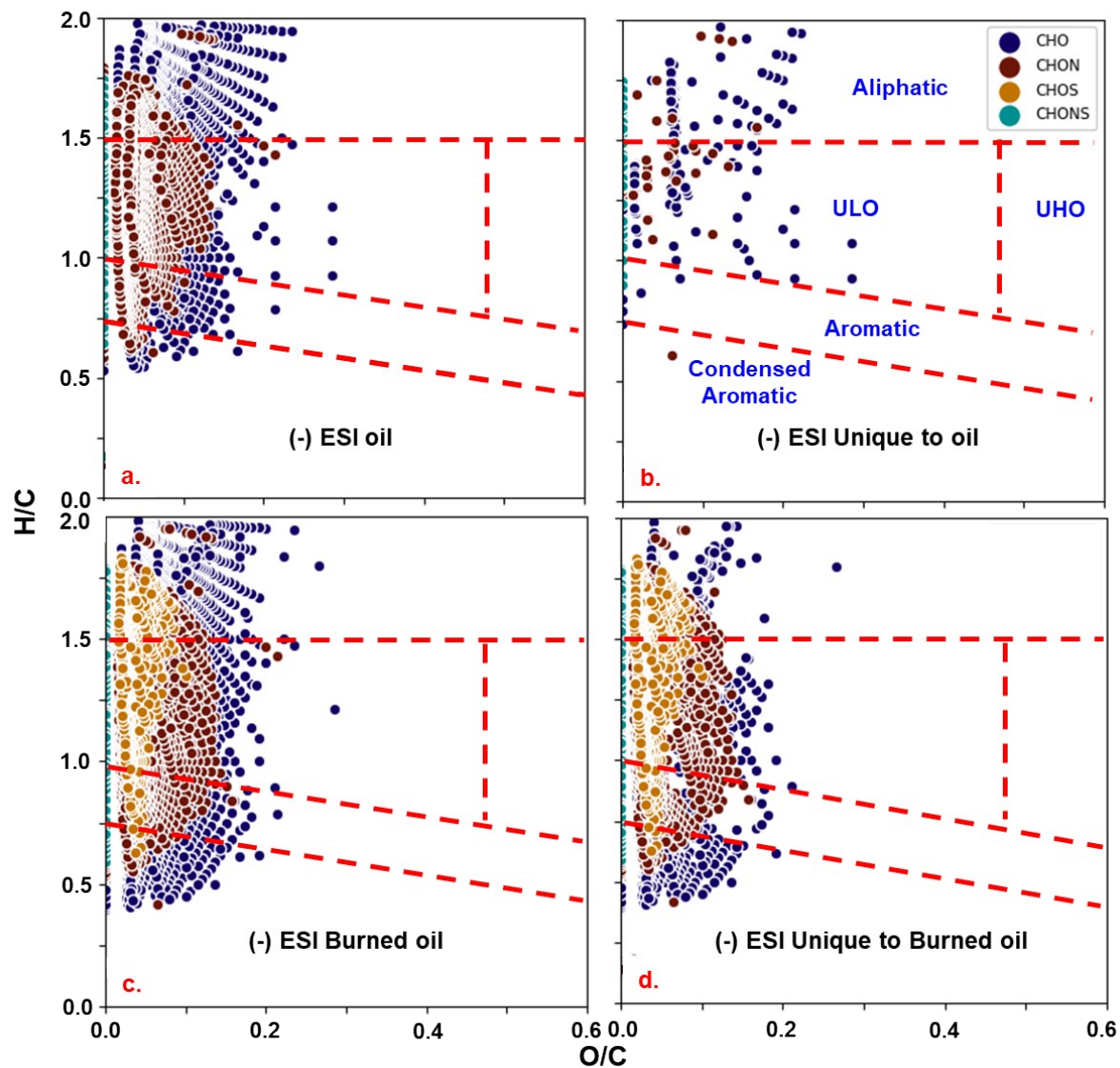


Figure S6: van Krevelen plots of H/C vs. O/C derived from FT-ICR MS showing assigned formulae for a) unburned oil, b) formulas unique to oil (in comparison to burned oil), c) burned oil, and d) formulas unique to burned oil (in comparison to unburned oil).

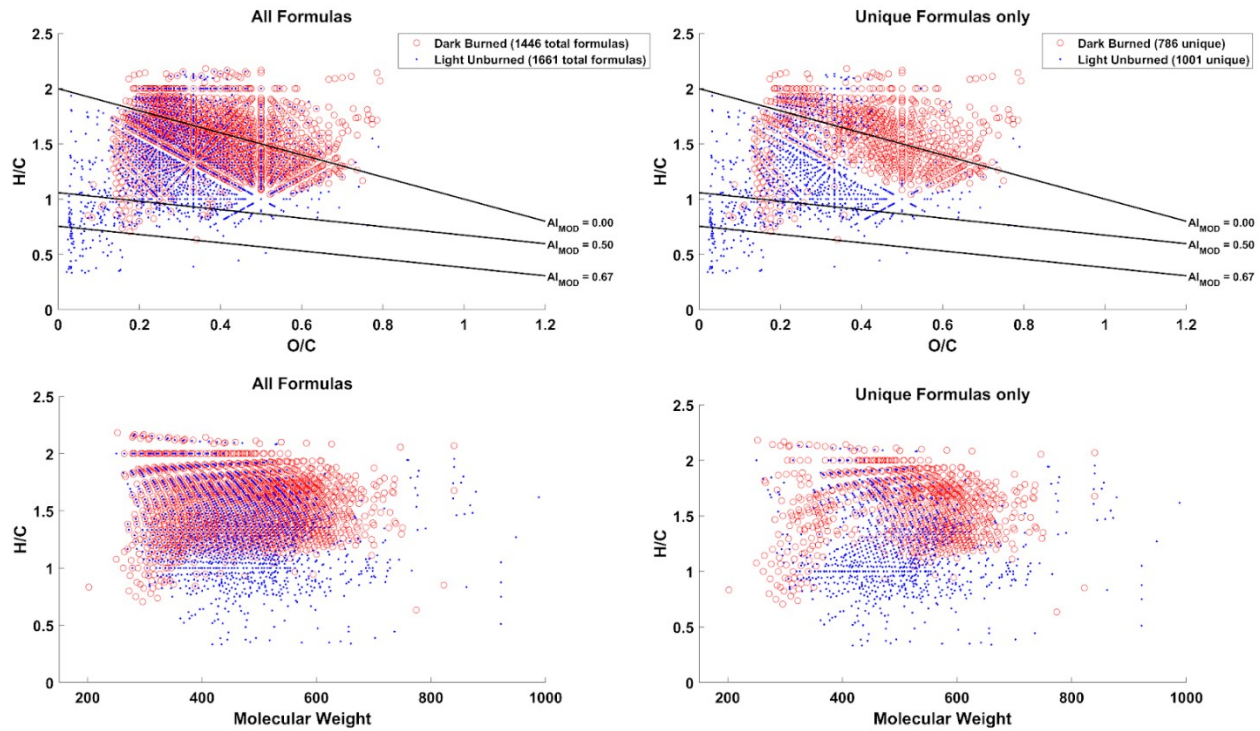


Figure S7. van Krevelen plots (top panels) and H/C vs. Molecular Weight plots (bottom panels) of CHOS formulas Dark Burned (red markers) and Light Unburned (blue markers). The right panels contain only the unique formulas, i.e., the 660 commonly shared formulas among the two samples are not shown for clarity.

Table S1: Classifications of WAF data derived from neg-ESI FT-ICR MS. Percentages are reported as relative abundances (RA %). Standard deviation (sd) for the darks was propagated based on the mean sd of all replicates for each class. CA = condensed aromatics, CRAM = carboxyl-rich alicyclic molecules, UHO = unsaturated high oxygen, ULO = unsaturated low oxygen.

Treatment	Aliphatic	Aromatic	CA	CRAM	UHO	ULO
Dark unburned	25.3 ± 2.2	2.68 ± 0.98	0.41 ± 1.91	47.6 ± 5.4	17.4 ± 1.4	6.65 ± 2.9
Light unburned	16.1 ± 2.5	16.4 ± 1.1	1.25 ± 0.41	44.4 ± 3.0	1.02 ± 0.38	20.8 ± 3.1
Dark burned	43.9 ± 2.2	0.77 ± 0.98	0.04 ± 1.91	42.4 ± 5.4	5.59 ± 1.40	7.35 ± 2.90
Light burned	10.5 ± 2.0	10.8 ± 0.9	4.32 ± 3.42	56.7 ± 7.8	6.96 ± 2.50	10.8 ± 2.

Table S2: Classifications of oil data derived from FT-ICR MS. Data were collected at the National High Magnetic Field Laboratory on a 9.4 T FT-ICR MS.

Sample	Aliphatic (%)	Aromatic (%)	CA (%)	UHO (%)	ULO (%)	Average Molecular Weight
Oil	16.9	19.5	2.4	0	61.2	448.2
Burned Oil	17.0	21.3	2.8	0	58.9	501.0

References

1. Kaiser, N.K., Savory, J.J., McKenna, A.M., Quinn, J.P., Hendrickson, C.L., Marshall, A.G., 2011. Electrically compensated Fourier transform ion cyclotron resonance cell for complex mixture mass analysis. *Anal. Chem.* 83, 6907-6910. doi: 10.1021/ac201546d.
2. Blakney, G. T.; Hendrickson, C. L.; Marshall, A. G., Predator data station: A fast data acquisition system for advanced FT-ICR MS experiments. *Int. J. Mass Spectrom.* 2011, 306 (2-3), 246-252. Doi: 10.1016/j.ijms.2011.03.009
3. Koch, B. P.; Dittmar, T., From Mass to Structure: An Aromaticity Index for High-Resolution Mass Data of Natural Organic Matter. *Rapid Commun. Mass Spectrom.* 2005, 20, 926-932. doi.org/10.1002/rcm.2386

4. Šantl-Temkiv, T.; Finster, K.; Dittmar, T.; Hansen, B. M.; Thyrhaug, R.; Nielsen, N. W.; Karlson, U. G., Hailstones: A Window into the Microbial and Chemical Inventory of a Storm Cloud. *PLoS One* 2013, 8 (1), e53550. doi.org/10.1371/journal.pone.0053550

5. Hemingway, J. D. Fourier transform: open-source tools for FT-ICR MS data analysis 2017-. <http://github.com/FluvialSeds/fouriertransform> (accessed 2018-05-29).